INTERNATIONAL SOCIETY FOR SOIL MECHANICS AND GEOTECHNICAL ENGINEERING



This paper was downloaded from the Online Library of the International Society for Soil Mechanics and Geotechnical Engineering (ISSMGE). The library is available here:

https://www.issmge.org/publications/online-library

This is an open-access database that archives thousands of papers published under the Auspices of the ISSMGE and maintained by the Innovation and Development Committee of ISSMGE.

The paper was published in the proceedings of the 20th International Conference on Soil Mechanics and Geotechnical Engineering and was edited by Mizanur Rahman and Mark Jaksa. The conference was held from May 1st to May 5th 2022 in Sydney, Australia.

Investigation of ground settlement due to dissipation of excess pore water pressure after liquefaction

Étude du tassement du sol dû à la dissipation de l'excès de pression interstitielle après liquéfaction

Bahareh Bahari & Tae-Hyung Kim

Department of Civil and Environmental Engineering, Korea Maritime and Ocean University, Republic of Korea, baharehbahari1989@gmail.com

ABSTRACT: Soil liquefaction may occur when the excess pore water pressure of saturated sandy soil is increased during an earthquake. The solidification process which occurs after liquefaction due to dissipation of excess pore water pressure causes permanent settlement in the ground. In this study, data from Nakdong river soil located in Busan City is used to simulate free field ground with 10-meter depth liquefiable sandy soil layer. In order to perform sensitivity analysis, three different sinusoidal motions with different amplitudes and frequencies are used to investigate the differences in the outcome. Throughout the three analysis cases, the excess pore water pressures at various depths and settlements are estimated. It is found that the secondary settlement due to the dissipation of the excess pore water pressure and solidification process is significantly greater (78% of final settlement at weakest motion case) than the initial settlement due to liquefaction and it should be considered in liquefaction analysis.

RÉSUMÉ: La liquéfaction du sol peut se produire lorsque la pression interstitielle excessive d'un sol sableux saturé augmente pendant un tremblement de terre. Le processus de solidification qui se produit après la liquéfaction en raison de la dissipation de la pression interstitielle excessive provoque un tassement permanent dans le sol. Dans cette étude, les données du sol de la rivière Nakdong situé dans la ville de Busan sont utilisées pour simuler un terrain en champ libre avec une couche de sol sableux liquéfiable de 10 mètres de profondeur. Afin d'effectuer une analyse de sensibilité, trois mouvements sinusoïdaux différents avec différentes amplitudes et fréquences sont utilisés pour étudier les différences dans le résultat. Dans les trois cas d'analyse, les pressions interstitielles excédentaires à diverses profondeurs et tassements sont estimées. On constate que le tassement secondaire dû à la dissipation de la pression interstitielle excessive et au processus de solidification est significativement plus élevé (78% de tassement final au cas de mouvement le plus faible) que le tassement initial dû à la liquéfaction et il doit être pris en compte dans l'analyse de liquéfaction.

KEYWORDS: Settlement; soil liquefaction; dissipation; excess pore water pressure; ground motion.

1 INTRODUCTION

Liquefaction may be observed in saturated loose sandy soils due to the increase of excess pore water pressure during a strong earthquake. This phenomenon can affect the settlement of soil deposits depending on the severity and characteristics of the earthquake motion. Many researchers have investigated the settlement characteristics of non-cohesive soil induced by cyclic loading over the past few decades. The generation of excess pore water pressure occurs as a consequence of earthquake motion and mostly in saturated sands (Lee and Albaisa 1974; Seed et al. 1975; Dobry et al. 1985; Cetin and Bilge 2011; Park et al. 2015; Porcino and Diano 2017, Chen et al. 2019). Figure 1 presents a schematic diagram of the time history of the excess pore water pressure ratio during an earthquake (Sumer 2011).

In a free field, the liquefaction occurs at shallow depths (Shahir and Pak 2010; Hasheminezhad and Bahadori 2019). Significant settlement could occur when there is excess pore water pressure or liquefaction (Ueng et al. 2010). Ishihara and Yoshimine (1992) and Tsukamoto and Ishihara (2010) proposed empirical methods for estimating the liquefaction-induced settlement in free field soil deposits. However, they did not consider the effect of excess pore water pressure dissipation that causes solidification and significant settlement in the ground.

It is essential to comprehend the post liquefaction behavior that causes secondary vertical displacement due to liquefaction induced by an earthquake. The aim of this study is to assess the seismic-induced settlement that occurs after liquefaction and solidification (compaction) process over time due to earthquake motion while considering the drainage conditions of the ground and the dissipation of excess pore water pressure.

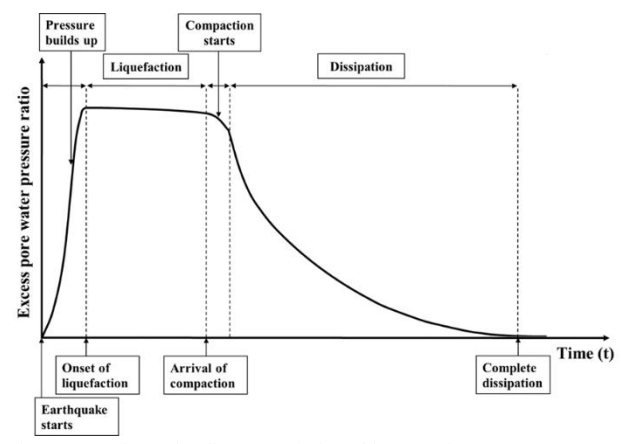


Figure 1. Schematic diagram of time history of excess pore water pressure ratio (Sumer 2011)

2 OUTLINE OF MODEL

Bahari et al. (2020) showed that the Nakdong River soil located In Busan, South Korea is highly vulnerable to liquefaction. Hence, the soil data from the Nakdong River was used in a finite element analysis. According to borehole data, the ground consists of 4 layers: sand, clay, sand, and weathered rock, which are up to 53 m deep. Figure 2 shows the typical particle size distribution curve of the soil.

The ground water table is 1 m from the ground surface. Data from geotechnical in-situ tests were used to simulate the

liquefaction resistance curve of the Nakdong River soil. Table 1 presents the properties of each soil layer.

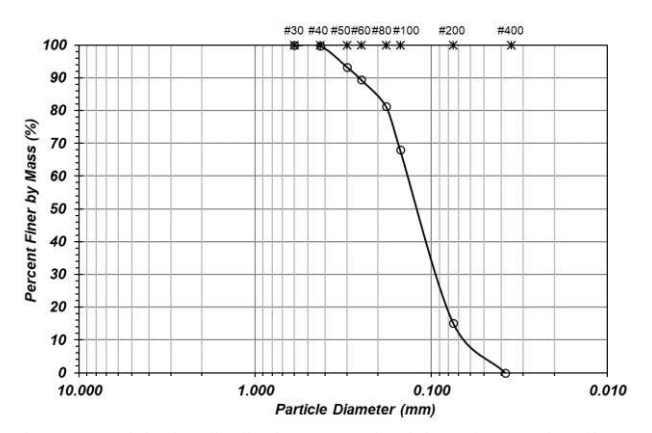


Figure 2. Particle size distribution curve of Nakdong river sandy soil

Table 1. Properties of each soil layer of Nakdong river

Title	Poisson ratio	Internal friction angle (°)	Permeability (m/s)
Liquefiable sand	0.33	30.0	0.0015
Clay	0.33	20.0	0.0001
Non-liquefiable sand	0.33	30.0	0.0001
Weathered rock	0.33	33.0	-

3 ANALYSIS CASES

The ground was subjected to three different damped sinusoidal loads as input motion with amplitudes of 0.15g, 0.31g, and 0.42g and frequencies of 1.5, 1.0, and 0.5 Hz, respectively. The loads were applied for 20 s in order to examine the excess pore water pressure generation and associated deformations due to seismic motion. Figure 3 illustrates the acceleration time history of three damped sinusoidal input motions.

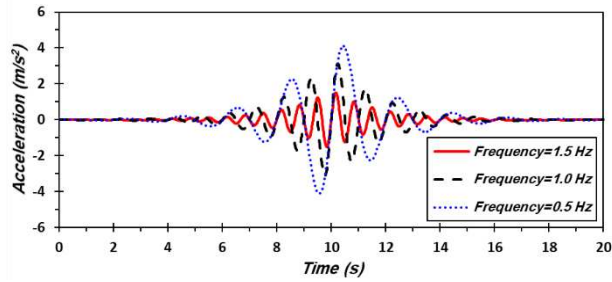


Figure 3. Acceleration time history of three sinusoidal input motions

Overall, there are 3 analysis cases with different drainage conditions, as shown in Table 2.

Table 2. Characteristics of analysis cases

Case No.	Motion frequency (Hz)	Amplitude (g)
Case 1	1.5	0.15
Case 2	1.0	0.31
Case 3	0.5	0.42

3.1 Two-dimensional finite element analysis

FLIP ROSE is a two-dimensional effective stress analysis program for evaluating damage and displacement induced by liquefaction (Iai et al., 1992). It is capable of analyzing the dissipation of excess pore water pressures based on a constitutive model (i.e., the cocktail glass model; Iai et al., 2011). FLIP ROSE was used to simulate the generation and dissipation of excess pore water pressure and the initial and permanent displacement induced by liquefaction due to moderate to severe ground motions.

There are two programs associated with FLIP ROSE called FLIPSIM and FLIPCSIM. These preprocessors are used for element simulation to define the liquefaction characteristic targets for undrained and drained conditions, respectively. The outcome of mentioned preprocessors is used in the main FLIP ROSE analysis. Figure 4 illustrates the measured and estimated liquefaction resistance curves of Nakdong River sand. The general cross section of the finite element model is shown in Figure 5.

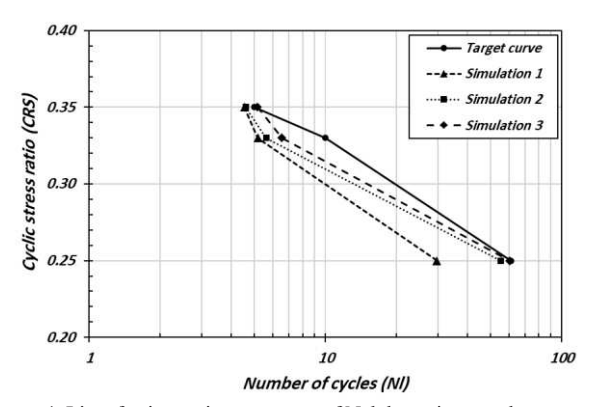


Figure 4. Liquefaction resistance curve of Nakdong river sand

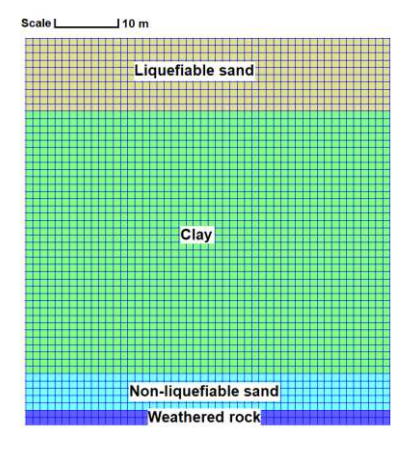


Figure 5. General cross section of the finite element model

4 RESULTS AND DISCUSSIONS

Figure 6 illustrates the initial settlement due to the generation of excess pore water pressure for case 1 at different soil depths. The results are from the beginning of motion until the peak of motion at 15 s. Figure 7 presents the secondary settlement due to dissipation of excess pore water pressure for case 1 at different soil depths from the peak of motion (15 s) until the end of the analysis (36,020 s).

In this case, the final settlement for the first layer at the end of the motion is about 1.13 cm, which is about 47% of the final settlement at the end of the analysis. The final settlement of the

first layer is about 2.38 cm at the end of the analysis. The settlement of the first layer at t=15 s is about 0.9. The settlement became stable around t=8900 s, but before that, the slope of the increase in settlement over time is high. The settlement for the last layer (d=10 m) is about 1 cm.

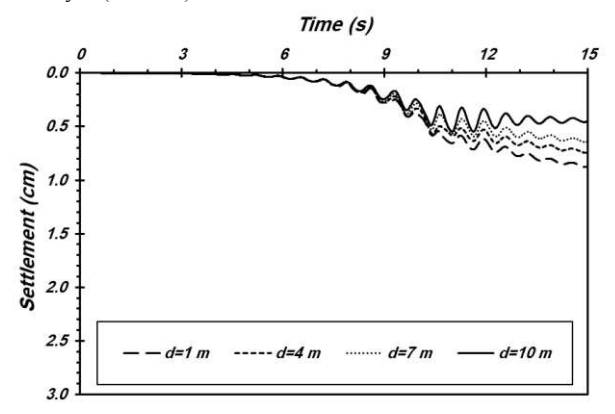


Figure 6. Settlement for case 1 for drained condition at different soil depths from the beginning till the peak of the motion

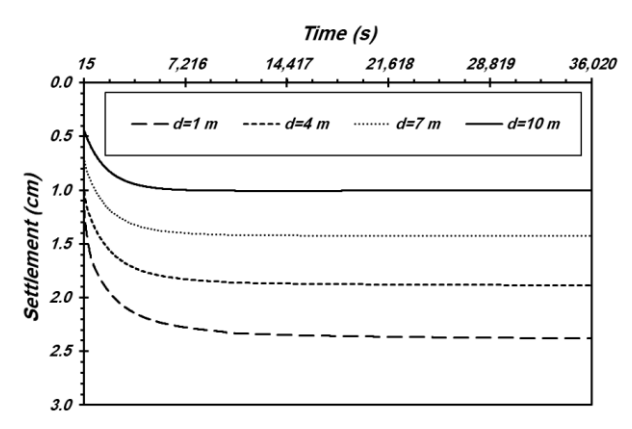


Figure 7. Settlement for case 1 for drained condition at different soil depths from the peak of the motion till the end of the analysis

Figure 8 shows the time history of the excess pore water pressure ratio for case 1 for the period of 0-15 s. The maximum ratio occurs at about 9-12 s when the peak motion occurs, and it rises until 0.92 at the first layer. Blue arrows indicating the starting point of the compaction process are shown for depths of 4.5, 6.5, and 9.5 m. The compaction starts at about t=13.2 s at the bottom layer.

Figure 9 presents the excess pore water pressure for case 1 from the peak of motion until the end of the analysis. The excess pore water pressure ratio reaches 0.8 at the first layer at the end of motion. It is found that the excess pore water pressure ratio has not decreased by the end of the motion. The time needed for full dissipation of the excess pore water pressure is about 660 s for the first layer.

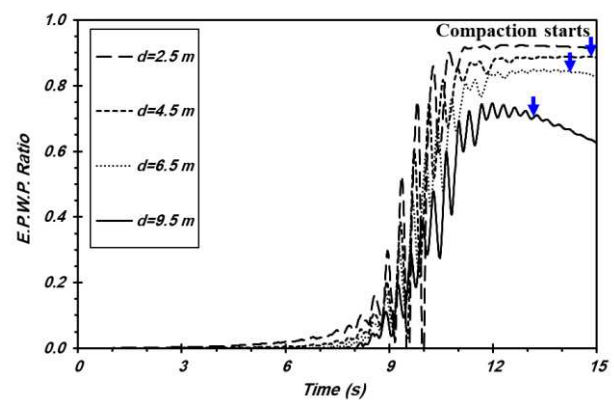


Figure 8. Time history of excess pore water pressure ratio for case 1 from the beginning till the peak of the motion

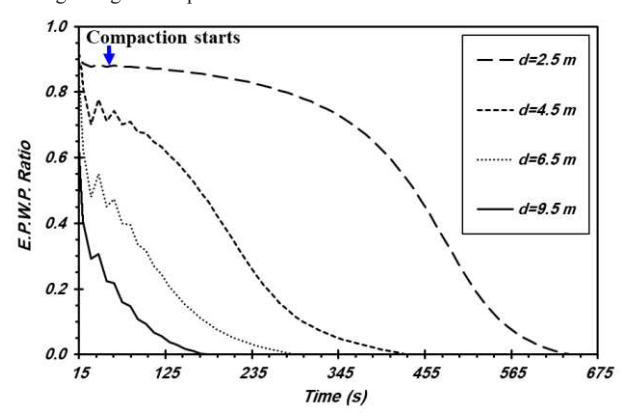


Figure 9. Time history of excess pore water pressure ratio for case 1 from the peak of the motion till the end of the analysis

The starting point of the compaction process is indicated in Figure 9 at about 60 s. This figure demonstrates the way that the excess pore water pressure ratio dissipates at different depths.

Figure 10 illustrates the settlement due to the generation and dissipation of excess pore water pressure for case 2 at different soil depths. For case 2, where the motion frequency is 1.0 Hz, the final settlement at the first layer is about 5.9 cm (147% higher than case 1). The rate of increase in the settlement of first layer is high until 8040 s and is almost 96% of the total settlement. In this case, the minimum settlement, which occurs at the bottom layer (d=10 m), is about 2.8 cm.

At the end of the motion, the initial settlement is about 1.2 cm and 2.0 cm at bottom layer and first layer, respectively. Comparing the settlement at the first layer for case 1, the 0.5-Hz decrease in motion frequency (1.0 Hz) causes greater settlement, particularly for the post liquefaction settlement when the excess pore water pressure ratio is fully dissipated. The initial settlement at first layer at t=20 s shows a 78% increase for case 2 compared to case 1.

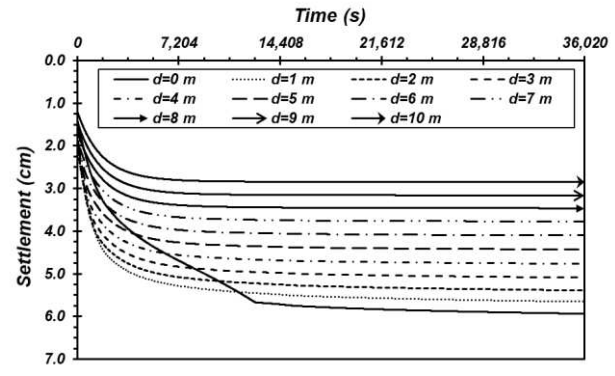


Figure 10. Settlement for case 2 at different soil depths

Figure 11 presents the excess pore water pressure for case 2. The excess pore water pressure ratio for case 2 reaches 0.95 at the first layer, and by the end of motion, it has decreased to 0.86. Moreover, almost all layers are still liquefied by the end of the motion in case 2. The excess pore water pressure ratio dissipates faster at the bottom layers, and the dissipation process starts upward from the bottom layers. At d=9.5 m, it takes about 780 s for the excess pore water pressure to fully dissipate. For the first layer (d=1.5 m), the excess pore water pressure dissipation process takes 1800 s.

Figure 12 illustrates the settlement due to the generation and dissipation of excess pore water pressure for case 3 at different soil depths. In case 3, with a frequency of 0.5 Hz, the settlement due to post liquefaction is significantly increased. The final settlement of the first layer is about 13.8 cm at the end of the analysis (a 134% increase compared to case 2). The initial settlement at the end of the motion is 2.3 cm at the first layer, which is notable since it was negligible in previous case. Therefore, analysis under drained conditions considering post-liquefaction settlement shows a more critical result for ground settlement. The bottom layer (d=10 m) has 6.9 cm of settlement at the end of the analysis.

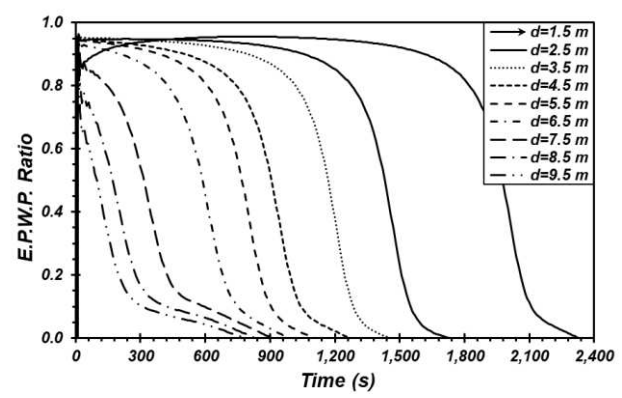


Figure 11. Time history of excess pore water pressure ratio for case 2

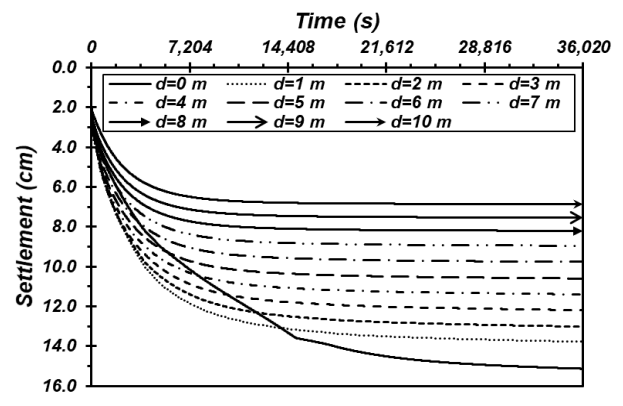


Figure 12. Settlement for case 3 at different soil depths

Figure 13 illustrates the settlement due to the generation and dissipation of excess pore water pressure for case 3 at different soil depths. In this case, the excess pore water pressure ratio rises to 0.97 around t=11 s, which is the highest value among the cases. At the end of the motion, it is 0.96 at the first layer and 0.88 at the bottom layer.

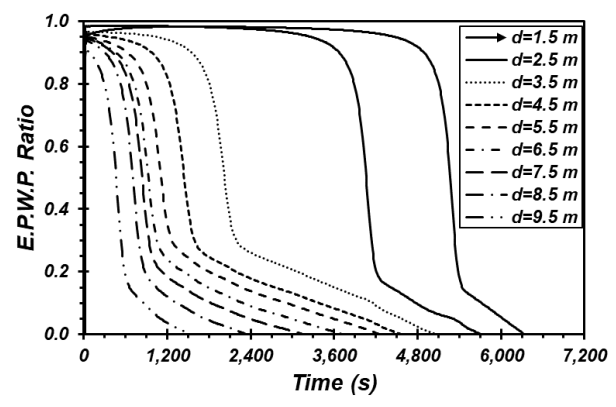


Figure 13. Time history of excess pore water pressure ratio for case 3

Figure 14 illustrates the distribution of excess pore water pressure ratio for case 3 at the end of motion. Similar to case 2, all layers are in a liquefied state by the end of the motion. It takes about 5700 s for the excess pore water pressure ratio to fully dissipate at the first layer. There is a 216% increase in the time needed for the excess pore water pressure to fully dissipate compared to case 2. At the bottom layer, the dissipation time for the excess pore water pressure ratio is 1680 s, which shows a 115% increase compared to case 2.

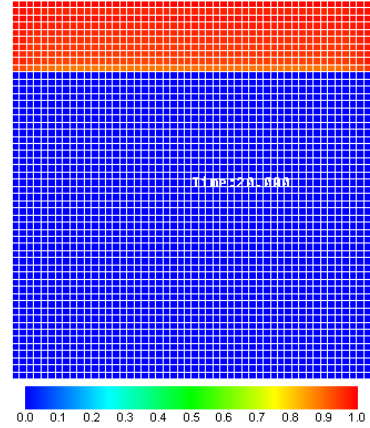


Figure 14. Distribution of excess pore water pressure ratio for case 3 at the end of motion

The process of excess pore water pressure dissipation for case 3 is presented in Figure 15. Figure 15(a) captures a cross section of the analysis model at the end of motion. From the first layer to d=9 m, all layers are liquefied, and at the last layer, the excess pore water pressure ratio is about 0.8. Figure 15(b) shows the results from 25 min after the motion. At t=1520 s, the excess pore water pressure has dissipated at bottom layers until d=4 m.

Figure 15(c) shows that after 50 min of motion, the top 3 m is still liquefied, while the other layers clearly show the excess pore water pressure has dissipated. Figure 15(d) presents the model after 75 min. In this stage, the excess pore water pressure at the top 2 m has not been dissipated yet. In Figure 15(e), only the first layer is liquefied. Finally, Figure 15(f) shows the model at t=17,720 s, when all excess pore water pressure has fully dissipated.

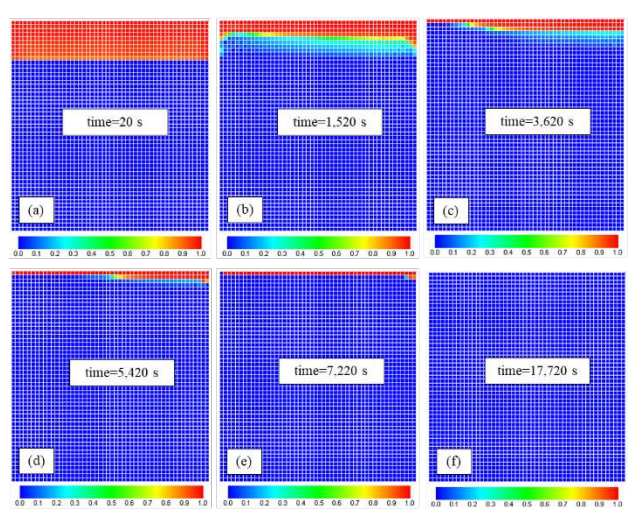


Figure 15. Process of excess pore water pressure dissipation for case 10

5 CONCLUSIONS

Earthquake-induced liquefaction is one of the most disastrous phenomena and could create significant displacements in the ground. To date, researchers have mostly considered the initial displacement. A free-field dynamic response analysis was carried out through finite element analysis to study the differences between the settlement induced by the generation and dissipation of excess pore water pressure. This study presented the results of 3 analysis cases with 10-m-deep liquefiable soil, and three different motion properties.

- 1. The secondary settlement that occurs due to dissipation of excess pore water pressure was more significant than the initial one that occurs during the motion. In the weakest motion case, the secondary settlement is 78% of the total settlement. This demonstrates how disastrous the secondary settlement due to excess pore water pressure dissipation can be.
- 2. With a motion frequency of 1.5 Hz, soil layers higher than 5.5, 4.5, and 3.5 m deep became almost liquefied at the peak of the motion due to the increase in excess pore water pressure. At the end of the motion, only the first layer (d=1.5 m) for case 1 was in a liquefied state, and the excess pore water pressure ratio was decreased for the other cases.
- 3. For case 2, with motion frequencies of 1.0 Hz, soil layers higher than 7.5, 6.5, and 5.5-m deep were almost in a liquefied state at the peak of the motion. However, soil layers higher than 7.5 m deep were in a liquefied state at the end of the motion. With a motion frequency of 0.5 Hz for case 3, all soil layers were liquefied at the peak of the motion. Even at the end of the motion, all soil layers were liquefied, and the excess pore water pressure was not decreased.

4. The excess pore water pressure dissipation started from deeper layers and propagated upward. The time needed for the excess pore water pressure to fully dissipate was investigated for each case. Reducing the motion frequency from 1.5 Hz to 1.0 Hz led to the dissipation time of excess pore water pressure becoming 2.7 times larger. Finally, reducing the motion frequency from 1.0 Hz to 0.5 Hz caused the dissipation time to be 3.2 times longer.

6 REFERENCES

- Bahadori H., Motamedi H., Hasheminezhad A., Motamed R. 2020. Shaking table tests on shallow foundations over geocomposite and geogrid-reinforced liquefiable soils, *Soil Dyn. and Earthq. Eng.* 128 105896. https://doi.org/10.1016/j.soildyn.2019.105896.
- Bahari B., Hwang W., Kim T-H., Song Y-S. 2020. Estimation of liquefaction potential in Eco-Delta City (Busan) using different approaches with effect of fines content. *Geo-Engineering*. (11), 14. https://doi.org/10.1186/s40703-020-00121-4.
- Cetin K.O., Bilge H.T. 2011. Cyclic large strain and induced pore pressure models for saturated clean sands. *J. Geotech. Geoenviron. Eng.* 138 (3): 309–323. https://doi.org/10.1061/(ASCE)GT.1943-5606.0000631.
- Chen G., Zhao D., Chen W., Juang C.H. 2019. Excess Pore-Water Pressure Generation in Cyclic Undrained Testing, *J. of Geotech. and Geoenviron.* Eng. (ASCE). 145(7). https://doi.org/10.1061/(ASCE)GT.1943-5606.0002057.
- Chen G.X., Zhou Z.L., Sun T. Wu Q., Xu L.Y., Khoshnevisan S., Ling D.S. 2019. Shear modulus and damping ratio of sand-gravel mixtures over a wide strain range. *J. Earthquake Eng.* 1–34. https://doi.org/10.1080/13632469.2017.1387200.
- Dobry R., Pierce W.G., Dyvik R., Thomas G.E., Ladd R.S. 1985. Pore pressure model for cyclic straining of sand. *Research Rep.* Troy, NY: Rensselaer Polytechnic Institute.
- Hasheminezhad A., Bahadori H. 2019. Seismic response of shallow foundations over liquefiable soils improved by deep soil mixing columns. *Comput. Geotech.* 110: 251–273.
- Iai S., Matsunaga Y., Kameoka T. 1992. Analysis of undrained cyclic behavior of sand under anisotropic consolidation. Soils and Found. 32(2): 16-20.
- Iai S., Tobita T., Ozutsumi O., Ueda K. 2011. Dilatancy of granular materials in a strain space multiple mechanism model. *Int. J. Numer. Anal. Methods Geomech.* 35(3): 360-392.
- Ishihara K., Yoshimine M. 1992. Evaluation of settlements in sand deposits following liquefaction during earthquakes. *Soils Found*. 32(1): 173–88.
- Lee K.L., Albaisa A. 1974. Earthquake induced settlements in saturated sands. *J. Soil Mech. Found. Div.* 100 (4): 387–406.
- Park T., Park D., Ahn J.K. 2015. Pore pressure model based on accumulated stress. *Bull. Earthquake Eng.* 13 (7): 1913–1926. https://doi.org/10.1007/s10518-014-9702-1.
- Porcino D.D., Diano V. 2017. The influence of non-plastic fines on pore water pressure generation and undrained shear strength of sand-silt mixtures. *Soil Dyn. Earthq. Eng.* 101: 311–321. https://doi.org/10.1016/j.soildyn.2017.07.015.
- Seed H.B., Martin P.P., Lysmer J. 1975. The generation and dissipation of pore water pressures during soil liquefaction. *Berkeley, CA*: Univ. of California.
- Shahir H., Pak A. 2010. Estimating liquefaction-induced settlement of shallow foundations by numerical approach. *Comput. Geotech.* 37(3): 267–279.
- Sumer B.M. 2011. Liquefaction Around Marine Structures, WORLD SCIENTIFIC, 39–55. https://doi.org/10.1142/7986.
- Tsukamoto Y., Ishihara K. 2010. Analysis on settlement of soil deposits following liquefaction during earthquakes. *Soils Found.* 44(3): 399–411.
- Ueng T.S., Wu C.W., Cheng H.W., Chen C.H. 2010. Settlements of saturated clean sand deposits in shaking table tests. Soil Dyn. Earthq. Eng. 30(1): 50–60.